High-performance cavity-enhanced quantum memory with warm atomic cell

Lixia Ma
Shanxi University
Xing Lei
Shanxi University
Jieli Yan
Shanxi University
Ruiyang Li
Shanxi University
Ting Chai
Shanxi University
Zhihui Yan
Shanxi University https://orcid.org/0000-0002-7149-4939
Xiaojun Jia (jiaxj@sxu.edu.cn)
Shanxi University https://orcid.org/0000-0001-5499-5427
Changde Xie
Shanxi University
Kunchi Peng
Shanxi University

Article

Keywords: quantum information technology, optics, magnetometry

Posted Date: June 21st, 2021

DOI: https://doi.org/10.21203/rs.3.rs-568098/v1

Version of Record: A version of this preprint was published at Nature Communications on May 2nd, 2022.
See the published version at https://doi.org/10.1038/s41467-022-30077-1.

High-performance cavity-enhanced quantum memory with warm atomic cell

Lixia Ma[1,3], Xing Lei[1,3], Jieli Yan[1], Ruiyang Li[1], Ting Chai[1], Zhihui Yan[1,2*], Xiaojun Jia[1,2†], Changde Xie[1,2] & Kunchi Peng[1,2]

[1]State Key Laboratory of Quantum Optics Quantum Optics Devices, Institute of Opto-Electronics, Shanxi University, Taiyuan 030006, P. R. China

[2]Collaborative Innovation Center of Extreme Optics, Shanxi University, Taiyuan 030006, P. R. China

[3]These authors contributed equally: Lixia Ma, Xing Lei.

*e-mail:zhyan@sxu.edu.cn

†e-mail:jiaxj@sxu.edu.cn

High-performance quantum memory for quantized states of light is a prerequisite building block of quantum information technology. Despite great progresses of optical quantum memories based on interactions of light and atoms, physical features of these memories still can not satisfy the requirement for applications in practical quantum information systems, since all of them suffer from trade off between memory efficiency and excess noise. Here, we report a high-performance cavity-enhanced electromagnetically-induced-transparency memory with warm atomic cell in which a scheme of optimizing the spatial and temporal modes based on the time-reversal approach is applied. A quantum memory with the efficiency up to $78 \pm 1\%$ and the noise level close to quantum noise limit has been experimentally achieved. The realized quantum memory platform has been capable of preserving quantized optical states, and thus is ready to be applied in quantum information systems, such as distributed quantum logic gates and quantum-enhanced atomic magnetometry.

The high-performance quantum memory featuring both high memory efficiency and low excess noise is an indispensable building block in quantum physics, distributed quantum computation and quantum metrology. The multiple spatial separated macroscopic objects can be entangled by storing multipartite entangled state of optical modes. And multiple high efficiency quantum memories with noises at the quantum noise limit (QNL) are demanded, which can be used to store multipartite entangled state of optical modes [1, 2]. Constructing a large-scale quantum processor is challenging due to the existence of unavoidable decoherence in real-world quantum systems [3–5]. For scaling up the computational power, modular quantum processors provide a solution by integrating smaller quantum modules to a larger computing cluster. Modular quantum platforms are to keep smaller individual processing units, then connect them to one another via quantum entanglement among multiple quantum-network modules, and thereby implement more

complex quantum operations, such as distributed quantum logic gates [6, 7]. Enhancing the ability to entangle different modules (nodes) is significant for achieving such a modular approach, and its realizing depends on the memory fidelity of storing the multipartite entangled optical modes among quantum modules (nodes). In modular quantum architecture, the element registers of the distributed quantum logic gates can preserve, control and read out quantum states, which performs quantum operations. For example, the controlled-phase gates using a cluster-state resource of four quantum nodes are the building block of a one-way quantum computation. For implementing controlled-phase gates, the most basic requirement for storage of entangled state is to reduce the noises of high efficiency quantum memory to QNL, since only at this noise level one is able to preserve and distribute quantum states among nodes of processors; otherwise, the transmitted quantum information will be merged in the sea of noises. Besides, the atom-based measurement sensitivity ultimately is restricted by the QNL. Spin squeezing holds the promise to overcome this limit, and becomes a key strategy for precision measurements, including the improved sensitivity of atomic magnetometry [8, 9]. In quantum-enhanced atomic magnetometry, the spin squeezing can be generated by storing the squeezed optical mode, and then used to measure weak signal merged in the quantum noise, thus a high efficiency quantum memory at QNL is necessary [10].

Over the past decades, various light-atom interactions have been utilized to implement quantum memory, such as electromagnetically-induced-transparency (EIT) [11–16], far-off-resonance Raman [17], quantum non-demolition [18], Autler–Townes splitting [19] and photon echo interaction [20]. The high memory efficiency is crucially important for practical quantum information [21, 22]. Towards the aim of high efficiency, coherent optical memories based on strong EIT interactions have been achieved by using an optically dense cold atomic media [23]. The memory efficiency in warm atomic cell can also be improved by using optimal input signal mode [24]. The other main challenge for the memory of quantized optical states is to suppress the excess noise, which will destroy quantum features of stored states. In the processing of atom-light interaction with a Λ-type energy configuration, the coupling of the control mode on the signal mode transition will induce unwanted four-wave-mixing (FWM) noise, which is the main noise source of quantum memory [25]. In near-resonant EIT memory with the proper atomic number, the interaction strength for quantum memory is dominant and the influence of FWM noise is relatively less, thus the EIT memories are able to reach the QNL, which have been applied to preserve the squeezed light with atomic ensemble [26, 27]. However, the memory efficiencies in the completed experiments were lower than 23%, because the memory interactions are limited in order to

avoid unwanted excess noises [2, 27, 28]. Alternatively, optical cavity can enhance the light-atom interaction [29–35] and suppress the noise [36]. Optical cavity has been used as an intriguing approach to reduce the excess noises in quantum memory. Although the cavity-enhanced warm vapor scheme had been applied in the Raman memory to suppress FWM noises, the obtained memory efficiency was low for the requirement of practical applications [25]. Despite impressive progresses, so far, all completed atomic memories suffer from trade off between memory efficiencies and excess noises.

To accomplish quantum memory with the necessary features of both high memory efficiency and low excess noise, we present a cavity-enhanced EIT memory with warm atomic cell. For realizing high performance quantum memory, the optimal temporal and spatial modes matching technology is applied to implement the mode matching based on time-reversal approach [37]. In this way the FWM effect is off-resonance with the optical cavity and forbidden by destructive interference in the optical cavity, while the memeory interaction is enhanced with the assistance of resonating the signal mode with the optical cavity. Thanks to the cavity-enhanced EIT interaction and the perfect mode matching, the memory efficiency up to $78 \pm 1\%$ for the storage time of 100 ns and the excess noise close to QNL have been simultaneously achieved. The deterministic memory fidelity has reached 0.98 ± 0.01 for a single photon level coherent state, which exceeds the quantum no-cloning limit [38, 39]. For optical continuous-variable (CV) quantum information systems, the quantum information is encoded in the quadrature amplitudes and phases of optical signal modes, which have been used to implement quantum information protocols, such as quantum teleportation [40], quantum dense coding [41] and quantum dense metrology [42]. For the presented memory experiment of optical coherent state, the quantum information is also encoded and stored in the quadrature amplitudes and phases of optical signal modes. Besides, photons carrying information in discrete variable (DV), such as its arbitrary polarization state, can also be stored in the presented system by replacing the Glan-Thompson polarizer with a polarization insensitive beam splitter [43]. Thus, the cavity-enhanced memory works equally well for both CV and DV quantum information because the cavity-enhanced quantum memory is a linear mapping technique [44].

Results

Principle of cavity-enhanced quantum memory. In quantum optics, the optical mode is represented by the annihilation operator $\hat{a}$, the amplitude (phase) quadrature $\hat{X}_L$ ($\hat{Y}_L$) of light corresponds to the real (imaginary) part of the annihilation operator $\hat{a}$, as $\hat{X}_L = (\hat{a}+\hat{a}^\dagger)/\sqrt{2}$ ($\hat{Y}_L = (\hat{a} - \hat{a}^\dagger)/\sqrt{2}i$). Under the Holstein-Primakoff approximation, the collective atomic spin wave is described by the lowering operator $\hat{S} = \sum_i |g\rangle \langle m|$, amplitude (phase) quadrature $\hat{X}_A$ ($\hat{Y}_A$) of the atoms is associated with the y (z) component of the Stokes operator $\hat{S}_y$ ($\hat{S}_z$) on the Bloch sphere, which is represented by $\hat{X}_A = (\hat{S} + \hat{S}^\dagger)/\sqrt{2} = \hat{S}_y/\sqrt{\left\langle \hat{S}_x \right\rangle}$ ($\hat{Y}_A = (\hat{S} - \hat{S}^\dagger)/\sqrt{2}i = \hat{S}_z/\sqrt{\left\langle \hat{S}_x \right\rangle}$) [18]. The coherent state of light is a minimum uncertainty state with equal uncertainty between two conjugate quadrature components, which is usually used to describe the quantized state of laser. The quantum natures of an optical memory can be characterized by means of preserving coherent state, thus the coherent state of optical mode is utilized as the input state of quantum memory in our experiment. The quantized state can be transferred between light and atomic superposition in the EIT memory [16]. The Λ-type three-level system of a ground state $|g\rangle$, a meta-stable state $|m\rangle$ and an excited state $|e\rangle$ is employed in the EIT configuration, which is presented in the insert of Fig. 1 (a). The signal mode is near resonant with the transition between a ground state $|g\rangle$ and an excited state $|e\rangle$, while control mode is near resonant with the transition between a meta-stable state $|m\rangle$ and an excited state $|e\rangle$. In our system, the control mode is much stronger than the signal mode, and is treated as a classical mode. When the collective atomic spin wave $\hat{S}(t)$ interacts with the signal mode $\hat{a}(t)$ via EIT process, the quantized state of the signal mode and the atomic ensemble can be transferred to each other, because the effective Hamiltonian $\hat{H}_{EIT}$ of light-atom interaction is a type of beam-splitter interaction [45]. The quantum memory process include three stages of writing, storage, and reading which are implemented by modulating the light-atom interaction with a control mode. Therefore, the step-like function used as an approximation of switching on and off processes in EIT interaction can be shown as follows: $\hat{H}(t) = \hbar\kappa\hat{a}^\dagger\hat{S} + \hbar\kappa\hat{S}^\dagger\hat{a}$, $-\infty < t < 0$; $\hat{H}(t) = 0$, $0 < t < T_0$; $\hat{H}(t) = \hbar\kappa\hat{a}^\dagger\hat{S} + \hbar\kappa\hat{S}^\dagger\hat{a}$, $T_0 < t < \infty$, where $\kappa = \sqrt{N_a}\mu\Omega/\Delta$ is the effective light-atom interaction constant, N_a is the atomic number, μ is the light-atom coupling constant, Ω is the Rabi frequency of the control mode, and Δ is the detuning between light and atom coupling.

Fig. 1 (a) is a diagram for the cavity-enhanced quantum memory with a warm atomic cell. The cavity with a bow tie-type ring configuration consists of two plano mirrors and two concave

mirrors, which enables to enhance the light-atom interaction and suppress the excess noise. The input signal mode $\hat{A}(t)^{in}$ is coupled into the cavity mode $\hat{a}$ through the input-output mirror with the coupling rate to the cavity of input mode $\gamma_1 = T/(2\tau)$, where T is the transmissivity of input-output mirror and τ is the round-trip time of the optical mode inside optical cavity. The other three cavity mirrors are highly reflective for the signal optical mode, and one of them is mounted on piezoelectric transducer for scanning or locking the cavity length. When the input signal mode resonates with cavity mode and the control mode is near-resonance with the cavity mode, the FWM noise is off-resonance and effectively suppressed. The intracavity loss L is unavoidable in real experiment due to the imperfect coating, and the corresponding decay rate of intracavity loss is $\gamma_2 = L/(2\tau)$, which introduce the vacuum noise $\hat{A}(t)^{in}_{v}$. The atomic spin wave decoherence rate is γ_0, and couples the noise of atomic medium $\hat{S}(t)_{v}$ into cavity mode $\hat{a}$. Quantum Langevin equations, describing evolution of observable operators for the cavity mode $\hat{a}(t)$ and collective atomic spin wave $\hat{S}(t)$ are shown as

$$\frac{d\hat{a}(t)}{dt} = -\gamma\hat{a}(t) - i\kappa(t)\hat{S}(t) + \sqrt{2\gamma_1}\hat{A}(t)^{in} + \sqrt{2\gamma_2}\hat{A}(t)^{in}_{v}, \tag{1}$$

$$\frac{d\hat{S}(t)}{dt} = -\gamma_0\hat{S}(t) - i\kappa(t)\hat{a}(t) + \sqrt{2\gamma_0}\hat{S}(t)_{v}, \tag{2}$$

where $\gamma = \gamma_1 + \gamma_2$ corresponds the sum of the coupling rate and the decay rate of cavity. For an input signal mode to be stored, a complete mode expansion into the longitudinal modes of the input optical mode is expressed by $\hat{A}(t)^{in} = u(t)^{in}_0\hat{a}^{in}_0$, where $\hat{a}^{in}_0$ is an optical mode operator and $u(t)^{in}_0$ is a temporal mode function of the input optical mode, which determines the optical mode shape. The input mode is dynamically shaped in time to provide optimum memory efficiency, and the temporal mode function in our system is approximately described by a rising exponential function [37]. By solving quantum Langevin equations with the proper input temporal mode function, the memory efficiency $\eta(T_0)$ at the user-controlled storage time T_0 from input optical mode to stored-and-retrieved optical mode is given by [46]

$$\eta(T_0) = \frac{(-\gamma_1\gamma_0^2 e^{-\gamma T_0} + \gamma_1\kappa^2 e^{-\gamma_0 T_0})^2}{(\gamma_0+\gamma)^2(\kappa^2+\gamma_0\gamma)^2}. \tag{3}$$

Experimental realization of cavity-enhanced quantum memory. Fig. 2 (a) shows temporal variation of the experimentally measured photon fluxes by photoreceiver detector D1. The red line and the blue line indicate the photon fluxes of the input signal mode and the stored-and-retrieved mode that passed through the cavity-enhanced quantum memory system, respectively. In

experiment the memory efficiency is the ratio between the photon fluxes of stored-and-retrieved and input signal modes. From Fig. 2 (a), it can be seen that the memory efficiency has reached $78 \pm 1\%$, when the atomic cell is heated to around $95\ ^{\circ}\mathrm{C}$. The plot for memory efficiency v.s. storage time is shown in Fig. 2 (b). In our system, the buffer gas is filled in the cell to slow the atomic diffusion and reduce the time-of-flight broadening. The magnetic noise mainly limits the lifetime, and the lifetime in current memory system with warm atomic cell is $1.2\ \mu$s. Since quantum state can be preserved within the lifetime, the user-controlled storage time can be taken arbitrary value less than the lifetime, and is chosen as 100 ns in our experiment.

The quantum performance of cavity-enhanced memory is obtained by the time-domain balanced homodyne detector (BHD) measurement. Table 1 shows measured normalized excess noise of quadrature amplitudes (phases) and memory fidelity for different memory efficiencies, and all the results of the normalized excess noises are close to QNL. In the quantum memory, the fidelity $F = \{Tr[(\hat{\rho}_1^{1/2}\hat{\rho}_2\hat{\rho}_1^{1/2})^{1/2}]\}^2$, which describes the overlap of input states $\hat{\rho}_1$ and the states $\hat{\rho}_2$ released from the memory node, quantifies the performance of a quantum memory. The calculation details for the fidelity are given (see Supplemental Note 4). The quantum memory with unit fidelity can perfectly preserve quantum information of the input quantized states. From table 1, it can be seen that the excess noise of the quantum memory are almost independent of the memory efficiencies, that means the excess noise is effectively suppressed by the optical cavity. As well-known, the excess noises will degrade the memory fidelity, and only low excess noise enables to realize a high fidelity quantum memory. Our results have reached the deterministic memory fidelity of $F = 0.98 \pm 0.01$ for a weak input coherent state (the mean number of photons is 0.4), which surpass the quantum no-cloning limit of 2/3 [38, 39]. The presented quantum memory with high efficiency and low excess noise makes the possibility of preserving optical quantum states such as the squeezed light. The memory system with high efficiency and low excess noise has been able to be directly applied in executing quantum logic gates [6, 7] between quantum-network modules (nodes) connected in a small range and realizing sub-QNL atomic magnetometry [9].

Discussion

In conclusion, we experimentally demonstrate an cavity-enhanced EIT quantum memory with both high memory efficiency and low excess noise. Due to the use of an optical cavity with the optimal temporal and near-perfect spatial mode, the memory efficiency of $78 \pm 1\%$ and the excess

noise close to QNL have been simultaneously realized. Our scheme provides a promising solution for optimal quantum memory which is possible to realize near-unity deterministic memory fidelity. The intracavity loss limits the memory efficiency, and the reduction of the intracavity loss in this system will furthermore improve the memory performance. If the magnetic noise is reduced by optimizing the structure of magnetic shielding, the lifetime will be obviously increased. Alternatively, the cell-wall paraffin coating onto the inner surface of the cell provides an effective approach to extend the memory lifetime of warm atom in the cell, and the millisecond-scale lifetime in the paraffin coated cell can be reached by using rubidium and cesium atoms, respectively [9, 47]. If the magnetic shielding is optimized and paraffin-coated cell is employed as potential improvements, the current lifetime limitations can be overcome in future. The presented approach is achievable on a variety of other physical platforms, such as in trapped ions [48–51], superconductors [52–54], solid states [55–58] and optomechanics [59–63]. Quantized states of light, such as squeezing [64] and entanglement [65] are kernel resources in quantum information science and technology, and the cavity-enhanced quantum memory system performs well enough to preserve quantum information of arbitrary quantized optical states. Due to the experimental simplicity of a warm atomic cell setup [66, 67], the presented system is robust and easily controlled, which is ready to be applied in some quantum information systems.

Methods

Experimental setup. The experimental setup for implementing the cavity-enhanced quantum memory is shown in Fig. 1 (b), and the experimental details are given (see Supplemental Note 1). A ^{87}Rb atomic cell coated with 795 nm anti-reflection, which is placed in a magnetic shielding, is used as EIT medium of cavity-enhanced quantum memory system. An input signal mode with an optimized wave packet originally coming from Ti:sapphire laser is stored in an atomic cell inside the optical cavity. The time sequence of the cavity-enhanced quantum memory is given (see Supplemental Note 2). In this experiment, the photoreceiver detector D1 is applied to measure memory efficiency, which are theoretically analyzed in details (see Supplemental Note 3), and the excess noises can be analyzed from the time-domain BHD measurement.

Data Availability

The data that support the findings of this study are available from the corresponding author on request.

---

[1] Bachor H. A. & Ralph, T. C. *A Guide to Experiments in Quantum Optics* (Wiley-vch, Weinheim, Berlin, 2004).

[2] Yan, Z.-H., Wu, L., Jia, X.-J., Liu, Y.-H., Deng, R.-J., Li, S.-J., Wang, H., Xie, C.-D. & Peng, K.-C. Establishing and storing of deterministic quantum entanglement among three distant atomic ensembles. *Nat. Commun.* **8**, 718 (2017).

[3] Gottesman, D. & Chuang, I. L. Demonstrating the viability of universal quantum computation using teleportation and single-qubit operations. *Nature* **402**, 390-393 (1999).

[4] Jiang, L., Taylor, J. M., Sorensen, A. S. & Lukin, M. D. Distributed quantum computation based on small quantum registers. *Phys. Rev. A* **76**, 062323 (2007).

[5] Kok, P., Munro, W. J., Nemoto, K., Ralph, T. C., Dowling, J. P. & Milburn, G. J. Linear optical quantum computing with photonic qubits. *Rev. Mod. Phys.* **79**, 135 (2007).

[6] Daiss, S., Langenfeld, S., Welte, S., Distante, E., Thomas, P., Hartung, L., Morin, O. & Rempe, G. A quantum-logic gate between distant quantum-network modules. *Science* **371**, 614-617 (2021).

[7] Awschalom, D. et al. Development of Quantum Interconnects (QuICs) for Next-Generation Information Technologies. *PRX Quantum* **2**, 017002 (2021).

[8] Lvovsky, A. I., Sanders, B. C. & Tittel, W. Optical quantum memory. *Nat. Photon.* **3**, 706-714 (2009).

[9] Bao, H. et al. Spin squeezing of 10^{11} atoms by prediction and retrodiction measurements. *Nature* **581**, 159-163 (2020).

[10] Hald, J., Sorensen, J. L., Schori, C. & Polzik, E. S. Spin Squeezed Atoms: A Macroscopic Entangled Ensemble Created by Light. *Phys. Rev. Lett.* **83**, 1319 (1999).

[11] Fleischhauer, M. & Lukin, M. D. Dark-State Polaritons in Electromagnetically Induced Transparency. *Phys. Rev. Lett.* **84**, 5094 (2000).

[12] Eisaman, M. D., Andre, A., Massou, F., Fleischhauer, M., Zibrov, A. S. & Lukin, M. D. Electromagnetically induced transparency with tunable single-photon pulses. *Nature* **438**, 837-841 (2005).

[13] Chanelière, T., Matsukevich, D. N., Jenkins, S. D., Lan, S. Y., Kennedy, T. A. B. & Kuzmich, A.

Storage and retrieval of single photons transmitted between remote quantum memories. *Nature* **438**, 833-836 (2005).

[14] Choi, K. S., Deng, H., Laurat, J. & Kimble, H. J. The quantum internet. *Nature* **453**, 1023-1030 (2008).

[15] Vernaz-Gris, P., Huang, K., Cao, M., Sheremet, A. S. & Laurat, J. Highly-efficient quantum memory for polarization qubits in a spatially-multiplexed cold atomic ensemble. *Nat. Commun.* **9**, 363 (2018).

[16] Wang, Y.-F., Li, J.-F., Zhang, S.-C., Su, K.-Y., Zhou, Y.-R., Liao, K.-Y., Du, S.-W., Yan, H. & Zhu, S.-L. Efficient quantum memory for single-photon polarization qubits. *Nat. Photon.* **13**, 346-351 (2019).

[17] Ding, D.-S., Zhang, W., Zhou, Z.-Y., Shi, S., Shi, B.-S. & Guo, G.-C. Raman quantum memory of photonic polarized entanglement. *Nat. Photon.* **9**, 332-338 (2015).

[18] Hammerer, K., Sorensen, A. S. & Polzik, E. S. Quantum interface between light and atomic ensembles. *Rev. Mod. Phys.* **82**, 1041 (2010).

[19] Saglamyurek, E., Hrushevskyi, T., Rastogi, A., Heshami, K. & LeBlanc, L. J. Thermal-motion-induced non-reciprocal quantum optical system. *Nat. Photon.* **12**, 774-748 (2018).

[20] Cho, Y. W. et al. Highly efficient optical quantum memory with long coherence time in cold atoms. *Optica* **3**, 100 (2016).

[21] Varnava, M., Browne, D. E. & Rudolph, T. Loss Tolerance in One-Way Quantum Computation via Counterfactual Error Correction. *Phys. Rev. Lett.* **97**, 120501 (2006).

[22] Grosshans, F. & Grangier, P. Quantum cloning and teleportation criteria for continuous quantum variables. *Phys. Rev. A* **64**, 010301 (2001).

[23] Hsiao, Y. F. et al. Highly Efficient Coherent Optical Memory Based on Electromagnetically Induced Transparency. *Phys. Rev. Lett.* **120**, 183602 (2018).

[24] Novikova, I., Gorshkov, A. V., Phillips, D. F., Sorensen, A. S., Lukin, M. D. & Walsworth, R. L. Optimal Control of Light Pulse Storage and Retrieval. *Phys. Rev. Lett.* **98**, 243602 (2007).

[25] Saunders, D. J., Munns, J. H. D., Champion, T. F. M., Qiu, C., Kaczmarek, K. T., Poem, E., Ledingham, P. M., Walmsley, I. A. & Nunn, J. Cavity-Enhanced Room-Temperature Broadband Raman Memory. *Phys. Rev. Lett.* **116**, 090501 (2016).

[26] Honda, K., Akamatsu, D., Arikawa, M., Yokoi, Y., Akiba, K., Nagatsuka, S., Tanimura, T., Furusawa, A. & Kozuma, M. Storage and Retrieval of a Squeezed Vacuum. *Phys. Rev. Lett.* **100**, 093601 (2008).

[27] Appel, J., Figueroa, E., Korystov, D., Lobino, M. & Lvovsky, A. I. Quantum Memory for Squeezed Light. *Phys. Rev. Lett.* **100**, 093602 (2008).

[28] Cviklinski, J., Ortalo, J., Laurat, J., Bramati, A., Pinard, M. & Giacobino, E. Heralded Generation of

Ultrafast Single Photons in Pure Quantum States. *Phys. Rev. Lett.* **101**, 133601 (2008).

[29] Wu, H.-B., Gea-Banacloche, J. & Xiao, M. Observation of Intracavity Electromagnetically Induced Transparency and Polariton Resonances in a Doppler-Broadened Medium. *Phys. Rev. Lett.* **100**, 173602 (2008).

[30] Tanji, H., Ghosh, S., Simon, J., Bloom, B. & Vuletić, V. Elimination of the Diffraction of Arbitrary Images Imprinted on Slow Light. *Phys. Rev. Lett.* **103**, 043601 (2009).

[31] Cimmarusti, A. D., Yan, Z., Patterson, B. D., Corcos, L. P., Orozco, L. A. & Deffner, S. Environment-Assisted Speed-up of the Field Evolution in Cavity Quantum Electrodynamics. *Phys. Rev. Lett.* **114**, 233602 (2015).

[32] Vasilakis, G., Shen, H., Jensen, K., Balabas, M., Salart, D., Chen, B. & Polzik, E. S. Generation of a squeezed state of an oscillator by stroboscopic back-action-evading measurement. *Nat. Phys.* **11**, 389-392 (2015).

[33] Guerrero, A. M., Nussenzveig, P., Martinelli, M., Marino, A. M. & Florez, H. M. Quantum Noise Correlations of an Optical Parametric Oscillator Based on a Nondegenerate Four Wave Mixing Process in Hot Alkali Atoms. *Phys. Rev. Lett.* **125**, 083601 (2020).

[34] Bimbard, E., Boddeda, R., Vitrant, N., Grankin, A., Parigi, V., Stanojevic, J., Ourjoumtsev, A. & Grangier, P. Homodyne Tomography of a Single Photon Retrieved on Demand from a Cavity-Enhanced Cold Atom Memory. *Phys. Rev. Lett.* **112**, 033601 (2014).

[35] Yang, S.-J., Wang, X.-J., Bao, X.-H. & Pan, J.-W. An efficient quantum light-matter interface with sub-second lifetime. *Nat. Photon.* **10**, 381-384 (2016).

[36] Heller, L., Farrera, P., Heinze, G. & de Riedmatten, H. Cold-Atom Temporally Multiplexed Quantum Memory with Cavity-Enhanced Noise Suppression. *Phys. Rev. Lett.* **124**, 210504 (2020).

[37] He, Q.-Y., Reid, M. D., Giacobino, E., Cviklinski, J. & Drummond, P. D. Dynamical oscillator-cavity model for quantum memories. *Phys. Rev. A* **79**, 022310 (2009).

[38] Grosshans, F. & Grangier, P. Quantum cloning and teleportation criteria for continuous quantum variables. *Phys. Rev. A* **64**, 010301(R) (2001).

[39] Braunstein, S. L., Fuchs, C. A., Kimble, H. J. & van Loock, P. Quantum versus classical domains for teleportation with continuous variables. *Phys. Rev. A* **64**, 022321 (2001).

[40] Huo, M.-R., Qin, J.-L., Cheng, J.-L., Yan, Z.-H., Qin, Z.-Z., Su, X.-L., Jia, X.-J., Xie, C.-D. & Peng, K.-C. Deterministic quantum teleportation through fiber channels. *Sci. Adv.* **4**: eaas9401 (2018).

[41] Jing, J.-T., Zhang, J., Yan, Y., Zhao, F.-G., Xie, C.-D. & Peng, K.-C. Experimental Demonstration of

Tripartite Entanglement and Controlled Dense Coding for Continuous Variables. *Phys. Rev. Lett.* **90**, 167903 (2003).

[42] Steinlechner, S., Bauchrowitz, J., Meinders, M., Muler-Ebhardt, H., Danzmann, K. & Schnabel, R. Quantum-dense metrology. *Nat. Photon.* **7**, 626-630 (2013).

[43] Xu, Z.-X. et al. Long Lifetime and High-Fidelity Quantum Memory of Photonic Polarization Qubit by Lifting Zeeman Degeneracy. *Phys. Rev. Lett.* **111**, 240503 (2013).

[44] Hedges, M. P., Longdell, J. J., Li, Y.-M. & Sellars, M. J. Efficient quantum memory for light. *Nature* **465**, 1052-1056 (2010).

[45] Ou, Z.-Y. Efficient conversion between photons and between photon and atom by stimulated emission. *Phys. Rev. A* **78**, 023819 (2008).

[46] Yan, Z.-H., Liu, Y.-H., Yan, J.-L. & Jia, X.-J. Deterministically entangling multiple remote quantum memories inside an optical cavity. *Phys. Rev. A* **97**, 013856 (2018).

[47] Jensen, K. et al. Quantum memory for entangled continuous-variable states. *Nat. Phys.* **7**, 13-16 (2011).

[48] Langer, C. et al. Long-Lived Qubit Memory Using Atomic Ions. *Phys. Rev. Lett.* **95**, 060502 (2005).

[49] Casabone, B., Friebe, K., Brandstatter, B., Schuppert, K., Blatt, R. & Northup, T. E. Enhanced Quantum Interface with Collective Ion-Cavity Coupling. *Phys. Rev. Lett.* **114**, 023602 (2015).

[50] Hucul, D., Inlek, I. V., Vittorini, G., Crocker, C., Debnath, S., Clark, S. M. & Monroe, C. Modular entanglement of atomic qubits using photons and phonons. *Nat. Phys.* **11**, 37-42 (2014).

[51] Wang, Y., Um, M., Zhang, J.-H., An, S. M., Lyu, M., Zhang, J.-N., Duan, L.-M., Yum, D. & Kim, K. Single-qubit quantum memory exceeding ten-minute coherence time. *Nat. Photon.* **11**, 646-650 (2017).

[52] Sillanpaa, M. A., Li, J., Cicak, K., Altomare, F., Park, J. I., Simmonds, R. W., Paraoanu, G. S. & Hakonen, P. J. Autler-Townes Effect in a Superconducting Three-Level System. *Phys. Rev. Lett.* **103**, 193601 (2009).

[53] Flurin, E., Roch, N., Pillet, J. D., Mallet, F. & Huard, B. Superconducting Quantum Node for Entanglement and Storage of Microwave Radiation. *Phys. Rev. Lett.* **114**, 090503 (2015).

[54] Abdumalikov, A. A., Astafiev, O., Zagoskin, A. M., Pashkin, Y. A., Nakamura, Y. & Tsai, J. S. Electromagnetically Induced Transparency on a Single Artificial Atom. *Phys. Rev. Lett.* **104**, 193601 (2010).

[55] Clausen, C., Bussières, F., Afzelius, M. & Gisin, N. Quantum Storage of Heralded Polarization Qubits

in Birefringent and Anisotropically Absorbing Materials. *Phys. Rev. Lett.* **108**, 190503 (2012).

[56] Gündoğan, M., Ledingham, P. M., Almasi, A., Cristiani, M. & de Riedmatten, H. Quantum Storage of a Photonic Polarization Qubit in a Solid. *Phys. Rev. Lett*. **108**, 190504(2012).

[57] Ma, Y., Ma, Y.-Z., Zhou, Z.-Q., Li, C.-F. & Guo, G.-C. One-hour coherent optical storage in an atomic frequency comb memory. *Nat. Commun.* **12**, 2381 (2021).

[58] Zhong, M.-J., Hedges, M. P., Ahlefeldt, R. L., Bartholomew, J. G., Beavan, S. E., Wittig, S. M., Longdell, J. J. & Sellars, M. J. Optically addressable nuclear spins in a solid with a six-hour coherence time. *Nature* **517**, 177-180 (2015).

[59] Fiore, V., Yang, Y., Kuzyk, M. C., Barbour, R., Tian, L. & Wang. H.-L. Storing Optical Information as a Mechanical Excitation in a Silica Optomechanical Resonator. *Phys. Rev. Lett.* **107**, 133601 (2011).

[60] Safavi-Naeini, A. H., Mayer Alegre, T. P., Chan, J., Eichenmode, M., Winger, M., Lin, Q., Hill, J. T., Chang, D. E. & Painter, O. Electromagnetically induced transparency and slow light with optomechanics. *Nature* **472**, 69-73 (2011).

[61] Lee, H., Suh, M.-G., Chen, T., Li, J., Diddams, S. A. & Vahala, K. J. Spiral resonators for on-chip laser frequency stabilization. *Nat. Commun.* **4**, 2468 (2013).

[62] Riedinger, R., Hong, S. K., Norte, R. A., Slater, J. A., Shang, J. Y., Krause, A. G., Anant, V., Aspelmeyer, M. & Gröblacher, S. Non-classical correlations between single photons and phonons from a mechanical oscillator. *Nature* **530**, 313-316 (2016).

[63] Kiesewetter, S., Teh, R. Y., Drummond, P. D. & Reid, M. D. Pulsed Entanglement of Two Optomechanical Oscillators and Furry's Hypothesis. *Phys. Rev. Lett.* **119**, 023601 (2017).

[64] Zuo, X.-J., Yan, Z.-H., Feng, Y.-N., Ma, J.-X., Jia, X.-J., Xie, C.-D. & Peng, K.-C. Quantum Interferometer Combining Squeezing and Parametric Amplification. *Phys. Rev. Lett.* **124**, 173602 (2020).

[65] Zhou, Y.-Y., Yu, J., Yan, Z.-H., Jia, X.-J., Zhang, J., Xie, C.-D. & Peng, K.-C. Quantum Secret Sharing Among Four Players Using Multipartite Bound Entanglement of an Optical Field. *Phys. Rev. Lett.* **121**, 150502 (2018).

[66] Guo, J.-X., Feng, X.-T., Yang, P.-Y., Yu, Z.-F., Chen, L.-Q., Yuan, C.-H. & Zhang, W.-P. High-performance Raman quantum memory with optimal control in room temperature atoms. *Nat. Commun.* **10**, 148 (2019).

[67] Finkelstein, R., Lahad, O., Cohen, I., Davidson, O., Kiriati, S., Poem, E. & Firstenberg, O. Continuous Protection of a Collective State from Inhomogeneous Dephasing. *Phys. Rev. X* **11**, 011008 (2021).

Acknowledgments

The authors thank Luis A. Orozco for his helpful discussion. This research was supported by the Key Project of the National Key R&D program of China (Grant No. 2016YFA0301402), the National Natural Science Foundation of China (Grants No. 61775127, No. 61925503, No. 11904218, No. 11654002, and No. 11834010), the Program for the Innovative Talents of Higher Education Institutions of Shanxi, the Program for the Outstanding Innovative Teams of Higher Learning Institutions of Shanxi, the Program for Sanjin Scholars of Shanxi Province, and the fund for Shanxi "1331 Project" Key Subjects Construction.

Author contributions

Z.Y., X.J. and C.X. conceived the original idea. L.M., X.L., Z.Y., X.J. and K.P. designed the experiment. L.M., X.L., J.Y., R.L. and T.C. constructed and performed the experiment. L.M., X.L., Z.Y. and X.J. accomplished theoretical calculation and the data analysis. Z.Y., X.J., C.X. and K.P. wrote the paper. All the authors reviewed the manuscript.

Competing financial interests: The authors declare no competing financial interests.

Additional information

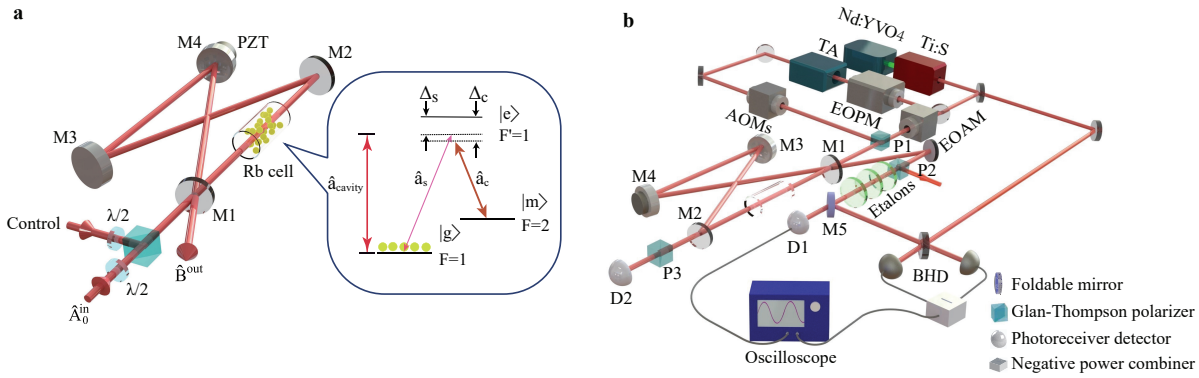

FIG. 1: **Schematic diagram.** **a** Diagram for the cavity-enhanced quantum memory and atomic energy level for quantum memory. Atoms with a ground state $|g\rangle$: $\left|5S_{1/2}, F=1\right\rangle$, a meta-stable state $|m\rangle$: $\left|5S_{1/2}, F=2\right\rangle$, and an excited state $|e\rangle$: $\left|5P_{1/2}, F'=1\right\rangle$ are shown. The atomic cell is placed between two plano mirrors, where the optical cavity simultaneously enhances the light-atom interaction and suppresses the excess noise. **b** Experimental setup for implementing cavity-enhanced quantum memory. TA: tapered amplifier; PZT, piezoelectric transducer; EOAM, electro-optical amplitude modulator; EOPM, electro-optical phase modulator; AOM, acousto-optical modulator; BHD, balanced homodyne detector.

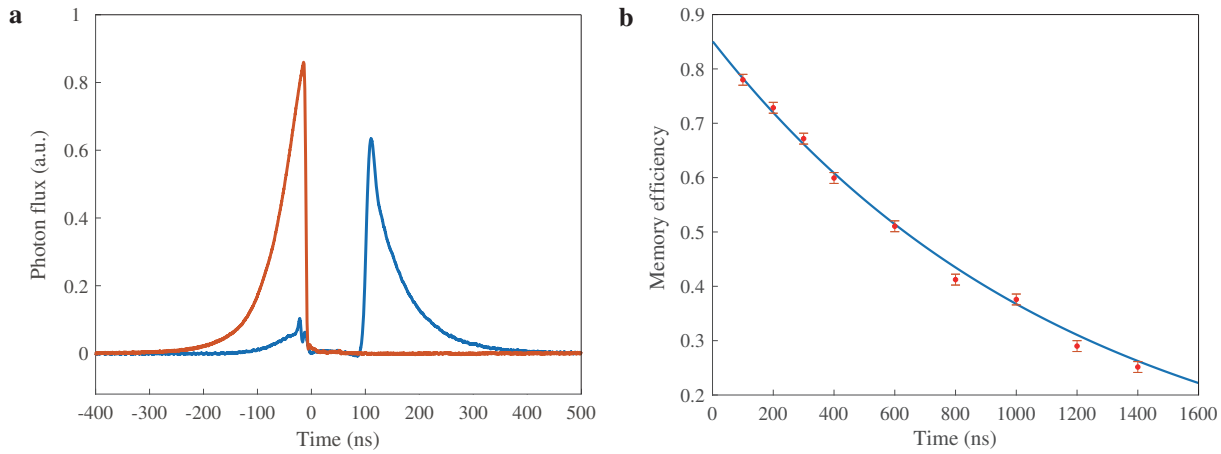

FIG. 2: **Experimental results.** **a** Temporal variation of the experimentally measured photon fluxes. The red line and the blue line indicate the photon fluxes of the input signal mode and the stored-and-retrieved mode, respectively. **b** The plot for memory efficiency v.s. storage time. Error bars represent $\pm 1\%$ standard error.

TABLE I: **Memory excess noise and memory fidelity v.s. memory efficiency.**

Memory efficiency	Normalized excess noise of quadrature amplitude	Normalized excess noise of quadrature phase	Memory fidelity
$61 \pm 1\%$	1.026 ± 0.02	1.025 ± 0.02	0.95 ± 0.01
$70 \pm 1\%$	1.025 ± 0.02	1.028 ± 0.02	0.97 ± 0.01
$78 \pm 1\%$	1.025 ± 0.02	1.027 ± 0.02	0.98 ± 0.01

Supplementary Files

This is a list of supplementary files associated with this preprint. Click to download.

- supplementary0527.pdf